

# Ultrathin Amorphous Carbon as Active Part of Vibrating MEMS †

Anne Ghis <sup>1,\*</sup>, Sébastien Thibert <sup>1</sup> and Marc Delaunay <sup>2</sup>

<sup>1</sup> LETI, CEA, Minatec Campus, Univ. Grenoble Alpes, F38000 Grenoble, France

<sup>2</sup> INAC-Pheliqs, CEA, Univ. Grenoble Alpes, 38000 Grenoble, France

\* Correspondence: anne.ghis@cea.fr; Tel.: +33-438-784-257

† Presented at the Eurosensors 2018 Conference, Graz, Austria, 9–12 September 2018.

Published: 4 December 2018

**Abstract:** Amorphous carbon in ultra-thin thicknesses shows amazing mechanical properties that make it particularly interesting for MEMS, especially as a vibrating membrane. We present the experimental results obtained on devices comprising composite membranes of a few nanometers thick suspended above cavities of 1 to 2  $\mu\text{m}$  in width. The behaviors in quasi-static mode—at low frequency—and also in resonant mode were observed and measured. Resonances frequencies of 20 MHz to 110MHz depending on the geometry were measured.

**Keywords:** MEMS; ultrasound; membrane; amorphous carbon; 2D material; report; resonance; AFM

---

## 1. Introduction

Ultrasound techniques are widely used as an analysis tool, in various fields, from medical imaging to materials science. The spatial resolution of the resulting information is related in particular to the geometry of the transducers. In the case of Micromachined Ultrasonic Transducers (MUT), the active part is a vibrating membrane operated at its natural frequency. The reduction of the vibrating surface of the devices to dimensions in the micrometer range is to be associated with a decrease in the thickness of the membrane to achieve functional displacements.

We present here preliminary studies [1] of MEMS devices having micrometer large vibrating area. An appropriate membrane material, a stamping transfer process and an original characterization setup have been implemented to produce natural resonant frequency measurements and discussion, and even allow the mapping of nodes and antinodes for higher order modes.

## 2. Materials and Methods

### 2.1. Device Description and Process

#### 2.1.1. Ultrathin Membrane Material

Reducing the thickness of the moving part to a few nanometer is a way to get significant amplitudes of vibration. It implies the use of a material having suitable flexibility and tenacity even in ultralow thicknesses. Amorphous carbon is a particular arrangement of carbon atoms between graphene and diamond that meets these mechanical criteria [2].

In this study, the amorphous carbon layer is coated by platinum on the one face and by nickel on the other face, in order to ensure electrical conductivity for capacitive actuation and for technological needs. The membrane material is therefore a three-layer metal/carbon/metal stack.

Two series of membranes differing in carbon thickness were studied, (referred to as A and B). The respective carbon thicknesses of A and B are  $3.7 \pm 0.3$  nm and  $8.1 \pm 0.3$  nm; platinum and nickel thicknesses are  $4.5 \pm 0.3$  and  $7.0 \pm 0.3$  nm. The three-layer stack is directly deposited onto a sacrificial PMMA layer using an Electron Cyclotron Resonance (ECR) process [3].

### 2.1.2. Device Realization

Each test chip was previously manufactured with a set of 0.8 to 2.3  $\mu\text{m}$  wide trenches (50 and 100  $\mu\text{m}$  long). The electrode set is designed for high frequency operation, top ground electrodes are patterned along the trench banks and signal electrodes are lying all along the bottom of the trenches, with vertical vias to connect surface coplanar pads.

The transfer operation is a stamping process (Figure 1): the platinum layer of the membrane stack is placed in contact with the surface of the test chip, and then the sacrificial layer is dissolved using acetone [1]. The three-layer stack lies onto the surface of the chip, locally suspended above the trenches, clamped on the trench banks, and electrically connected to the top ground electrodes. Contact pads are open through the membrane stack by a standard lithography process; during the removal of residual resins, the nickel layer protects the integrity of the carbon core of the stack.

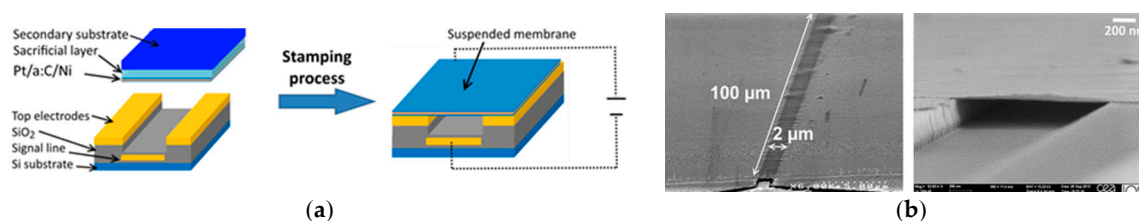


**Figure 1.** Realization of the devices (a) Scheme of the stamping process; (b) SEM pictures of membranes suspended above the trench.

### 2.2. Measurement Set Up

Devices are actuated by applying a voltage between signal and ground electrode. Amplitudes of deflection of the mobile part are measured using an AFM in tapping mode [1,4]. The AFM tip is coated with an insulator to avoid electrical contact between the equipment and the sample, the spring constant ranges from 1 to 7 N/m and the cantilever resonance frequency  $f_c$  is about 75 kHz.

When a DC voltage is applied, the suspended area may be scanned by the AFM tip and result in a static deflection mapping.

When a low frequency (i.e., the voltage generator frequency  $f_g \ll f_c$ ) voltage is applied, the AFM tip follows the deflection of the membrane. The local deflection versus time is recorded.

When a high frequency ( $f_g \gg f_c$ ) voltage is applied, the AFM tip does not follow the membrane displacements, it is repelled to an upper position and the actual measurement taken is the envelope of the membrane vibration. This configuration allows for measurements of the local amplitude of vibration depending on applied frequency, and spectrum analysis. More, when the applied signal fits with one of the resonance frequencies, and the AFM tip is set to scan an area, the resulting data build a map of nodes and antinodes.

## 3. Results

### 3.1. Low Frequency

At low frequencies, the displacement of the membrane instantly follows the applied voltage oscillations [5]. The amplitude of the displacement depends on the voltage swing (Figure 2).

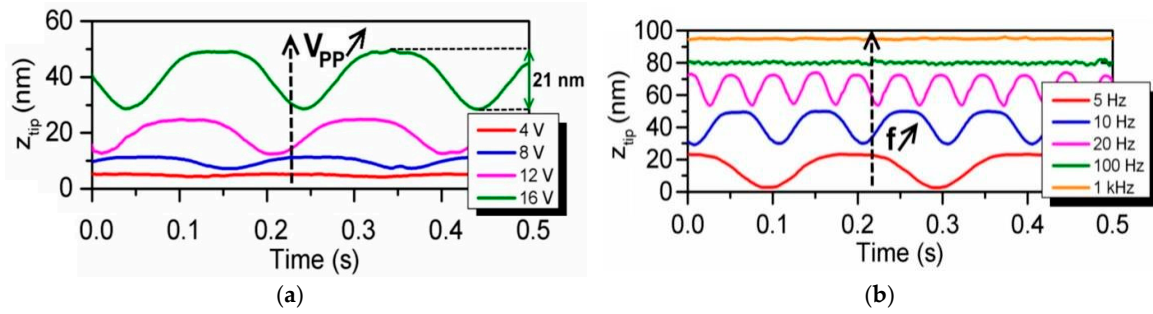


**Figure 2.** AFM Measurements of the displacement of a point of the membrane versus time at low frequency. (a) with frequency set at 5 Hz, and various AC voltage amplitudes; (b) with AC voltage amplitude set at 16 V, and various low frequencies. The operation of this measurement set up appears limited at frequencies lower than 100 Hz.

### 3.2. Frequency Spectrum

The study of vibration amplitudes as a function of frequency is carried out from 1 MHz and up to 110 MHz. For each value of the applied voltage, the displacement measured at 1 MHz—i.e., far from any resonance frequency—, is considered as the origin of the spectrum amplitudes.

A combination of DC bias ( $V_{dc}$ ) and AC excitation voltage ( $v_{ac}$ ) is applied to the samples. The instant resulting driving force is expressed by (1)

$$F_g(t) = A(z) \cdot (V_{dc} + v_{ac} \cos(2\pi f_g t))^2 = A(z) \cdot \left( \frac{V_{ac}^2}{2} + v_{ac}^2 + 2V_{dc}v_{ac}\cos(2\pi f_g t) + \frac{V_{ac}^2}{2} \cos(2(2\pi f_g t)) \right) \quad (1)$$

in which  $A(z)$  is a coefficient depending on the membrane displacement  $z$ , and  $f_g$  is the frequency of the AC excitation voltage.

For low AC excitation voltages, the resonance  $f_r$  clearly appears at  $f_r = f_g$  [16], (Figure 3)

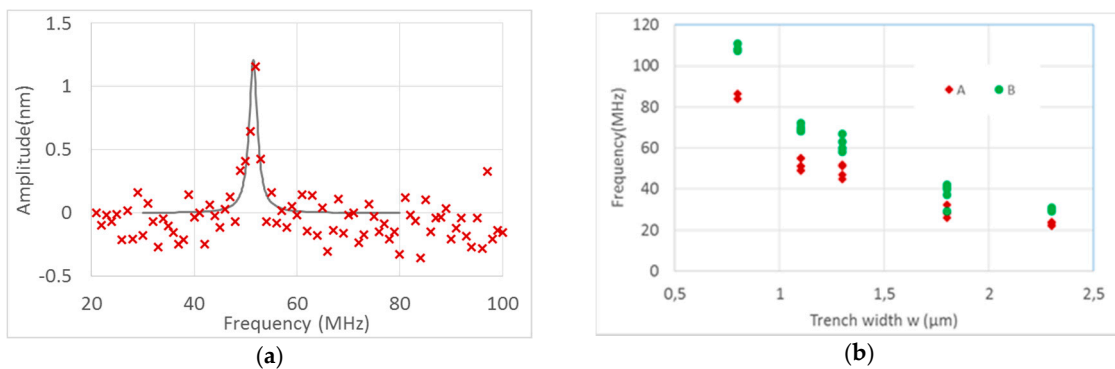


**Figure 3.** Natural resonance observation and measurement at low excitation level. AFM is used to measure the envelope of vibration of the membrane. (a) frequency spectrum taken on a 1.3  $\mu\text{m}$  wide sample device, with  $V_{dc} = 4$  V,  $v_{ac} = 0.5$  V. The resonant frequency appears to be  $f_0 = 52$  MHz; (b) resonance frequencies related to trench width for the two sets of devices differing by the thickness of amorphous carbon. Resonance frequencies range from 20 Hz for the 2.3  $\mu\text{m}$  wide trenches to 110 MHz for the 0.8  $\mu\text{m}$  wide trenches.

When AC voltages is increased ( $0.5 \text{ V} < v_{ac} < 5 \text{ V}$ ), the spectrum gets more complex (Figure 4a): harmonic resonance frequency peaks appear at  $f_g = 2f_r$ , and even at  $f_g = 3f_r$ . Peaks also appear at  $f_g = f_r/2$  and even  $f_g = 3f_r/2$ , corresponding to a membrane vibration frequency  $f_r = 2f_g$ . In addition, nonlinear phenomena such as duffing arise, inducing hysteresis and widening the resonance peaks. Very high amplitudes of deflection were measured around the main resonance peak. AFM scans taken on the vibrating area at different frequencies reveal nodes and antinodes location in accordance with high order transversal and longitudinal modes of resonance (Figure 4b) [1,7].

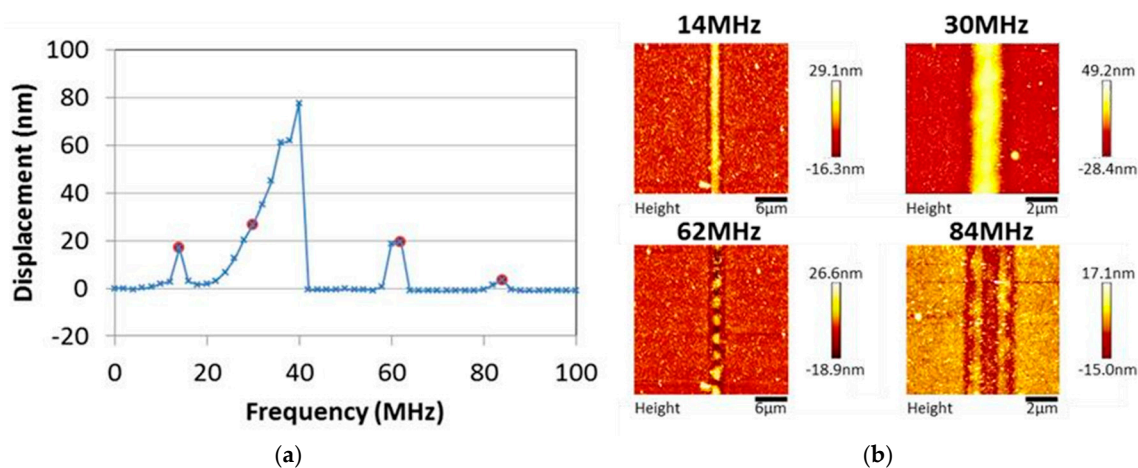


**Figure 4.** Resonances at high excitation of a 2.3  $\mu\text{m}$  wide device with a A-type membrane with natural frequency  $f_0 = 26$  MHz: (a) spectrum measured for  $V_{\text{dc}} = 15$  V,  $V_{\text{ac}} = 5$  V. Bullets indicate the frequencies corresponding to the scans shown in (b) Amplitude of vibration around 40 MHz is 80 nm on a 2.3  $\mu\text{m}$  large suspended width; (b) amplitude scans taken when biased with  $V_{\text{dc}} = 15$  V,  $V_{\text{ac}} = 5$  V at frequencies 14 MHz and 62 MHz on a 30  $\mu\text{m} \times 30 \mu\text{m}$  area, at frequencies 30 MHz on a 10  $\mu\text{m} \times 10 \mu\text{m}$  area, and at 84 MHz on a 8  $\mu\text{m} \times 8 \mu\text{m}$  area.

#### 4. Conclusions

Membranes made with ultrathin amorphous carbon as a core material and metal coating have demonstrated capacitive actuation, resonant behavior, and large deflection capabilities. They appear to be quite relevant for implementation as active part of vibrating MEMS.

**Author Contributions:** All three authors contributed to the device fabrication, the experiments, and the results analysis.

**Acknowledgments:** The authors acknowledge the financial support from the CEA's Nanosciences Transversal Program. This work has been performed with the help of the "Plateforme Technologique Amount" of Grenoble, with the financial support of the "Nanosciences aux limites de la Nanoélectronique" Foundation and CNRS Renatech network.

**Conflicts of Interest:** The authors declare no conflicts of interest.

#### References

1. Sébastien, T.; Delaunay, M.; Ghis, A. Carbon-Metal Vibrating Nanomembranes for High Frequency Microresonators. *Diamond Relat. Mater.* **2018**, *81*, 138–45, doi:10.1016/j.diamond.2017.12.005.
2. Luo, J.K.; Fu, Y.Q.; Le, H.R.; Williams, J.A.; Spearing, S.M.; Milne, W.I. Diamond and Diamond-like Carbon MEMS. *J. Micromech. Microeng.* **2007**, *17*, S147–S63, doi:10.1088/0960-1317/17/7/S12.
3. Delaunay, M.; Touchais, E. Electron Cyclotron Resonance Plasma Ion Source for Material Depositions. *Rev. Sci. Instrum.* **1998**, *69*, 2320–2324, doi:10.1063/1.1148938.
4. Suk, J.W.; Murali, S.; An, J.; Ruoff, R.S. Mechanical Measurements of Ultra-Thin Amorphous Carbon Membranes Using Scanning Atomic Force Microscopy. *Carbon* **2012**, *50*, 2220–2225, doi:10.1016/j.carbon.2012.01.037.
5. Thibert, S.; Ghis, A.; Delaunay, M. AFM Study of 2D Resonators Based on Diamond-Like-Carbon. In Proceedings of the 2016 IEEE 16th International Conference on Nanotechnology (IEEE-NANO), Sendai, Japan, 22–25 August 2016; pp. 479–82.

6. Lee, J.; Feng, P.X.-L. High Frequency Graphene Nanomechanical Resonators and Transducers. In Proceedings of the 2012 IEEE International Conference on Frequency Control Symposium (FCS), Baltimore, MD, USA, 21–24 May 2012; pp. 1–7,
7. Zhang, X.; Waitz, R.; Yang, F.; Lutz, C.; Angelova, P.; Götzhäuser, A.; Scheer, E. Vibrational Modes of Ultrathin Carbon Nanomembrane Mechanical Resonators. *Appl. Phys. Lett.* **2015**, *106*, 063107, doi:10.1063/1.4908058.



© 2018 by the authors. Licensee MDPI, Basel, Switzerland. This article is an open access article distributed under the terms and conditions of the Creative Commons Attribution (CC BY) license (<http://creativecommons.org/licenses/by/4.0/>).